



❖ Author's Choice

Assessing anesthetic activity through modulation of the membrane dipole potential

Benjamin Michael Davis,^{1,*} Jonathan Brenton,^{1,*} Sterenn Davis,^{*} Ehtesham Shamsheer,^{*} Claudia Sisa,^{*} Ljuban Grgic,^{*} and M. Francesca Cordeiro^{2,*†}

University College London Institute of Ophthalmology,^{*} London EC1V 9EL, United Kingdom; and Western Eye Hospital,[†] Imperial College Healthcare National Health Service Trust, and Imperial College Ophthalmic Research Group, Imperial College London, London NW1 5QH, United Kingdom

Abstract There is great individual variation in response to general anesthetics (GAs) leading to difficulties in optimal dosing and sometimes even accidental awareness during general anesthesia (AAGA). AAGA is a rare, but potentially devastating, complication affecting between 0.1% and 2% of patients undergoing surgery. The development of novel personalized screening techniques to accurately predict a patient's response to GAs and the risk of AAGA remains an unmet clinical need. In the present study, we demonstrate the principle of using a fluorescent reporter of the membrane dipole potential, di-8-ANEPPs, as a novel method to monitor anesthetic activity using a well-described inducer/noninducer pair. The membrane dipole potential has previously been suggested to contribute a novel mechanism of anesthetic action. We show that the fluorescence ratio of di-8-ANEPPs changed in response to physiological concentrations of the anesthetic, 1-chloro-1,2,2-trifluorocyclobutane (F₃), but not the structurally similar non-inducer, 1,2-dichlorohexafluorocyclobutane (F₆), to artificial membranes and in vitro retinal cell systems. Modulation of the membrane dipole provides an explanation to overcome the limitations associated with the alternative membrane-mediated mechanisms of GA action. Furthermore, by combining this technique with noninvasive retinal imaging technologies, we propose that this technique could provide a novel and noninvasive technique to monitor GA susceptibility and identify patients at risk of AAGA.—Davis, B. M., J. Brenton, S. Davis, E. Shamsheer, C. Sisa, L. Grgic, and M. F. Cordeiro. **Assessing anesthetic activity through modulation of the membrane dipole potential.** *J. Lipid Res.* 2017. 58: 1962–1976.

Supplementary key words cholesterol • diagnostic tools • eye • lipid rafts • model membranes • accidental awareness during general anesthesia • retina • di-8-ANEPPs • fluorescence spectroscopy

General anesthetics (GAs) are potent and reversible inducers of muscle relaxation, analgesia, immobility, reflex suppression, and sleep, without which many aspects of

modern medicine would be impossible. For this reason, GAs are widely considered to be one of the most important medical advances in the last 200 years. However, the mechanism of action of this diverse family of molecules remains poorly understood (1), as is the individual variation in patient response. This is an important problem, as a complete understanding of this mechanism will permit the design of molecules with improved safety and activity, and permit more accurate predictions of an individual's response to GA. Such an advance would contribute to developing better techniques to assess adequate levels of GA to administer and provide a personalized medicine approach to rapidly determine the best combination of GA agents for each patient. Furthermore, there is a risk of rare, but significant, complications presently associated with anesthetic administration, including malignant hyperthermia (2), succinylcholine-related apnea (3), anaphylaxis (4), accidental awareness during general anesthesia (AAGA) (5), and GA-associated mortality (6, 7).

AAGA is defined as the recall of events or experiences that occurred during anesthesia and is a potentially devastating complication affecting between 0.1% and 2% of all patients undergoing GA (8–10). Over three-quarters of the cases of AAGA are caused by a period of awareness under GA of less than 5 min duration. However, long-term adverse effects affect 41% of people with this condition (11). Patient recollection of AAGA range widely from nondistressing audiological recall to extremely distressing recollection of agony and paralysis, often associated with the development of posttraumatic stress disorder-like symptoms (10, 12). Multiple potential risk factors for AAGA have been identified by the recent NAP5 study, including the type of surgery (obstetric, cardiac, and pediatric), higher patient American Society of Anesthesiologists

This work was supported by a Medical Research Council Confidence in Concept Award to B.M.D. and M.F.C. and by a Swiss Study Foundation Scholarship and a University College London Overseas Research Scholarship to E.S. The authors declare no conflicts of interest.

*Author's Choice—Final version free via Creative Commons CC-BY license.

Manuscript received 2 December 2016 and in revised form 9 August 2017.

Published, JLR Papers in Press, August 17, 2017

DOI <https://doi.org/10.1194/jlr.M073932>

Abbreviations: AAGA, accidental awareness during general anesthesia; DCVJ, 9-(dicyanovinyl)julolidine; F₃, 1-chloro-1,2,2-trifluorocyclobutane; F₆, 1,2-dichlorohexafluorocyclobutane; GA, general anesthetic; MAC, minimum alveoli concentration; M β CD, methyl- β -cyclodextrin; PC, egg phosphatidylcholine.

¹B. M. Davis and J. Brenton contributed equally to this work.

²To whom correspondence should be addressed.

e-mail: M.Cordeiro@ucl.ac.uk

Copyright © 2017 by the American Society for Biochemistry and Molecular Biology, Inc.

This article is available online at <http://www.jlr.org>

score, and obesity (13). In addition, deficiencies in labeling and vigilance are also reported to contribute to AAGA (14) and an intrinsic (possibly genetic) resistance to GA has been suggested, with between 1.6% and 11% of patients reporting a previous history of AAGA (15, 16).

There is growing evidence to suggest that better monitoring of the depth of anesthesia can reduce the risk of AAGA (17). Depth of anesthesia is routinely monitored using the isolated forearm technique to measure the responsiveness to command as a consciousness surrogate, and quantifying the end-tidal concentration of volatile anesthetics or plasma levels of intravenously administered agents to assess anesthetic delivery (9). Each of these techniques, however, is of limited clinical utility, as only 50% of patients who respond to command with an isolated forearm can later recall doing so (9) and monitoring the extent of anesthetic delivery is not the same as monitoring the actual effectiveness of the GA (8). Alternative methods of monitoring response to anesthesia and measuring the level of consciousness include recording the electrical activity of the brain with evoked potentials and electroencephalograms. Despite the availability of these techniques for over 20 years (18), brain monitoring techniques are not routinely used in clinical practice. This is due to the difficulty in distinguishing brain activity from internal (muscular) and external (surgical device) interference, and different excitatory and inhibitory effects of GAs on different ion channels giving rise to complex electroencephalogram responses that can be further complicated by administration of non-GA drugs (8). As such, brain monitoring techniques are presently considered only qualitative indicators of GA depth (9, 19), meaning that there is a clear unmet need to develop techniques to accurately and quantitatively predict a patient's response to anesthesia.

The membrane dipole potential describes an electrical potential that arises from the organization of dipoles within and on the membrane surface [for a comprehensive review see (20)]. Ordinarily, the membrane dipole potential has a magnitude of between 200 and 400 mV, depending on membrane composition (21), and is independent of membrane fluidity (22). The dipole potential is also sensitive to cholesterol content (23) and stereospecificity (24) and can be used to modulate the activity of the raft-associated (25) membrane protein, P-glycoprotein (26–28). The theory of GA-mediated modulation of membrane dipole potential was first proposed by Qin, Szabo, and Cafiso (29). The authors reported that addition of 1 minimum alveoli concentration (MAC) equivalent concentrations of the GAs, enflurane, isoflurane, and halothane, to artificial membranes induced substantial reductions in the membrane dipole potential (−10.5, −10.5, and −6.7 mV, respectively). Other groups have also demonstrated that modulation of the membrane dipole potential can affect gramicidin A channel activity (30) [more recently with local anesthetics (31)] and sodium potassium pumps (32). Together, these data suggest that modulation of the membrane dipole potential could provide an attractive mechanism of indirect GA-induced modulation of membrane protein activity without requiring direct protein-ligand interactions.

The retina comprises the only portion of the CNS that can be readily visualized at the cellular level using noninvasive imaging techniques, such as confocal scanning laser ophthalmoscopy (33). Changes in retinal function have been reported using multifocal electroretinography, where isoflurane anesthesia induction in a porcine model resulted in a reduced RGC response (34). Building on this observation, we sought to determine the feasibility of monitoring retinal neuronal cell behavior in response to GA induction and whether this technique could ultimately be used to provide a screening tool to rapidly and quantitatively assess a patient's individual response to anesthesia prior to undergoing surgery. In the present study, we sought to determine whether the small molecule ratiometric probe, di-8-ANEPPs, which becomes strongly fluorescent only when incorporated into the cell membrane and has previously been used extensively to report on the membrane dipole potential (27, 28, 35), can be used to specifically report on anesthesia response using *in vitro* models. This was achieved by exposing di-8-ANEPPs-labeled artificial membrane (liposomes) and retinal neuronal cell lines to varying concentrations of either 1-chloro-1,2,2-trifluorocyclobutane (F_3) or 1,2-dichloro-hexafluorocyclobutane (F_6), an anesthetic/nonanesthetic pair with high structural similarity (Fig. 1) (36, 37). F_3 has been previously reported to inhibit presynaptic voltage-gated sodium channels and potentiate GABA_A chloride channels, while F_6 has been found to have no effect on either channel (38, 39). The di-8-ANEPPs was chosen for this purpose, as methods to convert the fluorescence ratio measured to quantitative membrane dipole potential changes are established (23). The ratiometric nature of di-8-ANEPPs also ensures that this measurement is independent of changes in partitioning of the probe between the membrane and aqueous milieu. The use of this probe with microscopic imaging techniques has been reported (40) and it is increasingly being used for *in vivo* applications (41). A proposed schematic for such a screening device for use in preoperative conscious patients measuring their unique responses to subclinical doses of GA or GA combinations is discussed.

METHODS

Reagents

All materials and reagents were acquired at the highest purity from Sigma-Aldrich (Kent, UK) unless otherwise stated. All statistical analyses were carried out using GraphPad Prism version 5.00 for Windows (GraphPad Software, San Diego, CA).

Unilamellar liposome preparation

Egg phosphatidylcholine (PC) and cholesterol (ovine) were purchased from Avanti Polar Lipids (Alabaster, AL). Liposomes were prepared using a lipid film hydration technique (42). Briefly, 13 mM of PC_{100%} or PC_{70%}Cholesterol_{30%} (molar ratios) were dissolved in a chloroform:methanol (5:1 ratio) solvent and dried under reduced pressure (50 mBar, 1 h at 45°C) to form a thin film. This film was rehydrated in sucrose-Tris buffer [280 mM sucrose, 10 mM Trizma-hydrochloride (pH 7.4), at 45°C for 1 h with agitation. The resulting liposome suspension was extruded

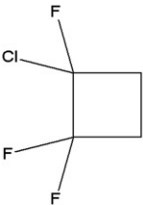
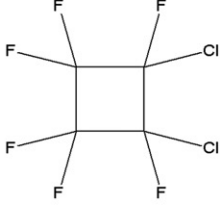
Property	1-Chloro-1,2,2-trifluorocyclobutane (F ₃)	1,2-Dichlorohexafluorocyclobutane (F ₆)
Structure		
Molecular Weight	144.521 g/mol	232.934 g/mol
LogP/ACD	0.54	1.68
Average molecular dipole	3.17 D	0.78 D

Fig. 1. Properties of the volatile anesthetic (F₃) and the nonimmobilizer (F₆). F₃ and F₆ possess similar lipophilicity [calculated using ACD/LogP (octanol/water partition coefficient) 12.0], but distinct average molecular dipoles (36), as a result of the more unequal distribution of electronegative halogen atoms in F₃ than in F₆.

sequentially through polycarbonate filters with pores of 400, 200, and 100 nm in diameter (Nucleopore Corp., Pleasanton, CA) using a handheld extruder (Mini-extruder; Avanti Polar Lipids) to produce a solution of unilamellar phospholipid vesicles of uniform size. Liposomes were labeled exclusively in the outer bilayer leaflet with di-8-ANEPPs, as described previously (27). Briefly, liposomes were incubated for 1.5 h at 37°C in the presence of di-8-ANEPPs (Thermo Fisher Scientific, Waltham, MA) dissolved in ethanol while protecting from light.

Liposome characterization by dynamic light scattering

Liposome size was determined using a Zetasizer Nano-ZS and Zetasizer 7.02 software (Malvern Instruments, Malvern, UK). Liposome suspensions were diluted to a concentration of 400 μM in sucrose-Tris buffer [280 mM sucrose, 10 mM Trizma-hydrochloride (pH 7.4), and particle size recorded prior to and following 5 mM additions of F₃ or F₆ using dynamic light scattering. The particle diameter (Z-average) and polydispersity of the liposome population were recorded for three populations, from which the average particle diameter was calculated.

Immortalized retinal neuronal cell culture

An immortalized retinal neuronal cell line (a gift from Dr. Neeraj Agarwal, Department of Cell Biology and Genetics, University of North Texas Health Science Center, Fort Worth, TX) was used in this study as a model neuronal cell. These neurons express the typical retinal and neuronal markers, Thy-1, Brn-3a, and β3 tubulin (43–45), and are also reported to have similarities to the 661W photoreceptor cell line (46–48). Retinal neurons were cultured in DMEM (Invitrogen, Paisley, UK) supplemented with 10% heat-inactivated fetal bovine serum (Invitrogen). Penicillin (100 U/ml) and streptomycin (100 mg/ml) were used to maintain the cells prior to experimentation.

The di-8-ANEPPs labeling of neuronal cell suspensions

Cell suspensions were counted using a trypan blue exclusion assay before harvesting by centrifugation (300 g, 5 min). Cells were labeled with di-8-ANEPPs according to the methods outlined by Asawakarn, Cladera, and O'Shea (28). Briefly, 10 μM of di-8-ANEPPs were added to a suspension of cells (1 × 10⁶ cells·ml⁻¹ sucrose-Tris buffer) for 1.5 h at 37°C with mixing. Labeled cells were used for experiments within 2 h of labeling. When required, depletion of cholesterol from cell membranes was achieved by treating di-8-ANEPPs cell suspensions for 1 min with 10 mM methyl-β-cyclodextrin (MBCD) before removal by centrifugation (300 g for

5 min at 25°C) and resuspension in fresh sucrose buffer. Cells were used for experiments within 1 h of cholesterol depletion.

Spectral and ratiometric fluorescent recordings

Fluorescence measurements were taken during the addition of the desired amounts of F₃, F₆, or primary alcohols to suspensions of liposomes or cells (400 μM lipid or 40,000 cells·ml⁻¹ sucrose-Tris buffer). Measurements were acquired on a Cary Eclipse fluorescence spectrophotometer (Agilent Technologies) and during acquisition samples were maintained at 37°C with magnetic stirring. Fluorescence difference spectra were obtained by subtracting the di-8-ANEPPs excitation spectra after the addition of agents of interest from those obtained at baseline. Before subtraction, each spectrum was normalized to the integrated areas so that the difference spectra would reflect only the spectral shifts (28). Each difference spectrum was then normalized to an appropriate buffer control and a three-point moving average applied to reduce noise.

The di-8-ANEPPs ratiometric time series were obtained using excitation wavelengths of 420 and 520 nm and an emission wavelength of 670 nm. Additions of 1, 2.5, or 5 mM of F₃ or F₆ were made after approximately 120 s of baseline recording and acquisition was continued until no further change in di-8-ANEPPs fluorescence signal was observed (typically between 300 and 600 s). Data were fit using linear regression (indicative of no significant change in di-8-ANEPPs ratio on addition of ligands) or plateau followed one-phase exponential decay function equation 1:

$$Y = IF \left\{ X < X_0, Y_0, \text{Plateau} + (Y_0 - \text{Plateau}) \times \exp[-K \times (X - X_0)] \right\} \quad (\text{Eq. 1})$$

where X₀ is the time at which the decay begins (fixed as the time of GA/non-GA addition), Y₀ is the average Y value at time X₀, plateau is the value of Y at infinite time, and K is the rate constant expressed as s⁻¹. The preferred model in each case was determined using an extra sum-of-squares F-test and the simpler model (linear regression) was selected, unless P < 0.05. The di-8-ANEPPs fluorescence ratios were converted into estimates of the membrane dipole potential using the calibration equation described by Starke-Peterkovic (23) (equation 2):

$$\psi_d = \frac{R + a}{b} \quad (\text{Eq. 2})$$

where ψ_d is the membrane dipole potential, R is the ratiometric intensity of di-8-ANEPPs fluorescence ratio, a = 0.3 (±0.4), and

$b = 4.3 (\pm 1.2) \times 10^{-3} \text{ mV}^{-1}$. In agreement with previous studies, as the large errors associated with a and b are thought to arise from difficulties in determining the absolute value of ψ_d and we were principally concerned with relative changes in ψ_d , only the variance in R was considered in error calculations (40).

Membrane fluidity measurements

Liposomes were labeled with the fluorescent probe, 9-(dicyanovinyl)julolidine (DCVJ), as described previously (49). Briefly, 13 mM PC_{100%} and PC_{70%}Cholesterol_{30%} liposomes were labeled with 45 μM DCVJ for 1.5 h at 37°C. Liposomes were diluted to 400 μM (1.5 μM DCVJ) with HEPES saline buffer [10 mM HEPES, 140 mM sodium chloride (pH 7.4)]. Fluorescence emission (490 nm) was recorded at an excitation of 430 nm during the addition of DMSO, F₃, and F₆. Measurements were acquired using a Cary Eclipse fluorescence spectrophotometer (Agilent Technologies) and during acquisition, samples were maintained at 37°C with magnetic stirring. Under the assumption of constant temperature and absorption, change in membrane fluidity (η_1/η_2) can be determined from DCVJ fluorescence emission on addition of DMSO, F₃, or F₆ using equation 3 (50);

$$\frac{\eta_1}{\eta_2} = \left(\frac{I_1 - I_0}{I_2 - I_0} \right)^{\frac{1}{x}} \quad (\text{Eq. 3})$$

where I_1 and I_2 are the fluorescence emission from DCVJ before and after addition of an agent that modulates membrane fluidity, x is a constant equal to 0.6 for DCVJ, and I_0 is the signal due to nonfluorescent scattering, filter bleed-through, and ambient light effects (here $I_0 = 110.23$).

Cell viability

An AlamarBlue resazurin reduction assay (Invitrogen) was conducted, as per the manufacturer's instructions, to measure the potential toxicity of all concentrations of anesthetic molecules used. Cells were incubated with the anesthetic compounds for 2 h at 37°C with 5% CO₂ and, following incubation, 10% AlamarBlue was added. A cell-free control containing 10% AlamarBlue only was included as a negative control. Fluorescence was measured on a Safire plate reader (Tecan, Zurich, Switzerland) with an excitation wavelength of 570 nm and an emission wavelength of 585 nm. Percentage viability was determined by normalization to untreated (100% viable) and cell-free control (0% viable) groups.

RESULTS

Addition of F₃, but not F₆, to liposomes induced a dose-dependent reduction in membrane dipole potential without membrane aggregation

Addition of 5 mM F₃ or F₆ to 400 μM PC_{100%} or PC_{70%}Cholesterol_{30%} liposomes did not induce significant liposome aggregation, retaining comparable average

population diameters and a polydispersity index of <0.2 in each case (Table 1 and Fig. 2). Titration of 1, 2.5, and 5 mM concentrations of F₃ into di-8-ANEPPs-labeled PC_{100%} and PC_{70%}Cholesterol_{30%} liposomes caused a concentration-dependent red-shift in the excitation spectrum (Fig. 3A, B), indicative of a reduction in the membrane dipole potential (27). The magnitude of the F₃-induced red-shift in the di-8-ANEPPs excitation spectra was reduced in PC_{70%}Cholesterol_{70%} versus PC_{100%} membranes, indicative of a smaller change in the membrane dipole potential in this membrane system. In contrast, no detectable spectral shift was recorded when liposomes were titrated with equivalent concentrations of the nonimmobilizer, F₆ (Fig. 3C, D).

Recording changes in di-8-ANEPPs 420/520 nm fluorescence ratio over time confirmed that addition of F₃ to PC_{100%} liposomes caused a concentration-dependent decrease in this parameter (Fig. 3D), while addition of equivalent concentrations of F₆ did not cause any apparent change (Fig. 3E). Titration of F₃ fit best to a plateau followed by single exponential decay function equation 1, while those involving F₆ typically best fit to a straight line function (indicative of no significant change in dipole potential) or exponential decay function with nominal span. Figure 3F illustrates that the change in dipole potential on addition of F₃ declined significantly and linearly with increasing concentration (F-test $P < 0.0001$ for PC_{100%}- and PC_{70%}Cholesterol_{30%}-containing liposomes), while the addition of F₆ had no such relationship (slope $\pm 95\%$ CI; PC_{100%} $0.39 \pm 4.06 \text{ mV/mM F}_6$ and PC_{70%}Cholesterol_{30%} $0.15 \pm 6.33 \text{ mV/mM F}_6$, F-test, $P = 0.82$ and $P = 0.95$, respectively). On comparing the gradient of each line, addition of F₃ to cholesterol-containing liposomes was found to induce a smaller change in the membrane dipole potential than addition to those comprised of PC alone (slope $\pm 95\%$ CI; PC_{100%} $-19.45 \pm 1.07 \text{ mV/mM F}_3$ vs. PC_{70%}Cholesterol_{30%} $-17.26 \pm 0.65 \text{ mV/mM F}_3$). Finally, the rate of dipole potential change on addition of F₃ to PC_{100%} liposomes was found to be almost twice that found on addition of this GA to PC_{70%}Cholesterol_{30%} membranes (Fig. 3G; $0.020 \pm 0.003 \text{ s}^{-1}$ vs. $0.013 \pm 0.002 \text{ s}^{-1}$, respectively, two-tailed unpaired t -test, $P = 0.0352$).

Addition of primary alcohols (ethanol to dodecanol), but no tetradodecanol, to liposomes induced a dose-dependent reduction in membrane dipole potential without membrane aggregation

The homologous series of primary alcohols between ethanol and dodecanol have long been established to possess increasing anesthetic potency with acyl chain length; however, between dodecanol and tetradodecanol, a cut-off point exists beyond which no anesthetic activity is observed (51). To investigate this phenomenon, the ability of

TABLE 1. Characteristics of liposomes in the presence or absence of F₃ and F₆

	PC _{100%}			PC _{70%} Cholesterol _{30%}		
	Naïve	Plus 5 mM F ₃	Plus 5 mM F ₆	Naïve	Plus 5 mM F ₃	Plus 5 mM F ₆
Z-average diameter (nm \pm SD)	142 (48)	144 (57)	141 (46)	163 (64)	164 (57)	163 (57)
Polydispersity index	0.099	0.110	0.060	0.105	0.088	0.084

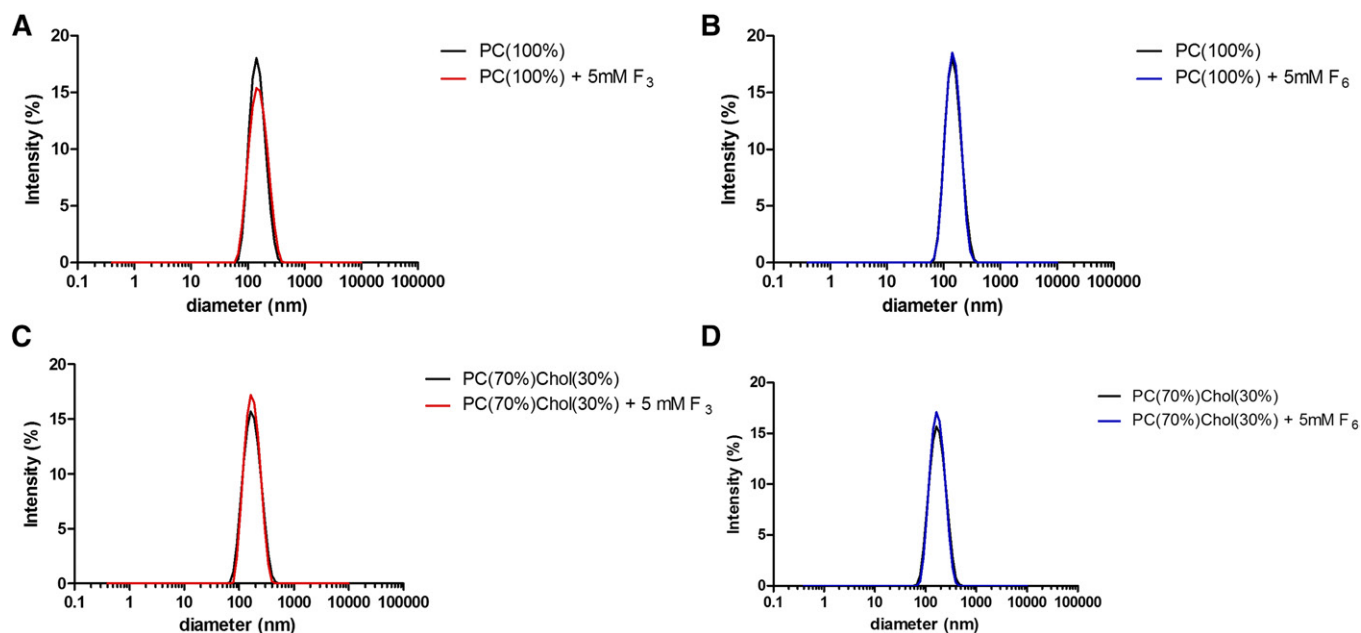


Fig. 2. Addition of 5 mM F_3 or F_6 did not induce liposome aggregation. Dynamic light scattering demonstrates that addition of 5 mM F_3 (A, C) or F_6 (B, D) did not induce significant aggregation of PC_{100%} (A, B) and PC_{70%}Cholesterol_{30%} (C, D) liposomes after incubation for 30 min at 37°C ($n = 3$).

primary alcohols to modulate the membrane dipole potential in PC_{100%} artificial membranes was investigated (Fig. 4). Titration of primary alcohols with an acyl chain length between 2 and 12 carbons was found to induce a dose-dependent reduction in the membrane dipole potential (Fig. 4C–I), with the concentration required to induce a 5% reduction in dipole potential (~ 18 mV) reducing with increasing acyl chain length (Fig. 4A). The concentration of primary alcohols required to induce a reduction in membrane dipole potential significantly correlated (Fig. 4B; slope = 0.9618 ± 0.09172 , Spearman's $R = 0.964$, $P = 0.0028$) with the EC_{50} of these molecules previously reported in tadpoles (51, 52). Titration of membranes with tetradodecanol, however, did not induce a significant change in membrane dipole potential up to concentrations of 0.17 mM (Fig. 4J) with addition of greater concentrations of this alcohol, including visible precipitation in the cuvette.

Addition of F_3 and F_6 to DCVJ-labeled artificial membrane systems induces a small, but physiologically irrelevant, increase in membrane fluidity

As the fluorescence emission of DCVJ is dependent on the dielectric constant of its environment (49), the effective labeling of membranes with DCVJ was first assessed by recording the fluorescence emission spectra (Fig. 5A). Peak emission wavelength was observed at 487 nm for both membrane compositions, which is similar to that previously reported for PC-containing liposomes (49). A positive control to confirm the efficacy of this technique was the addition of DMSO (0.5% v/v to 2% v/v) to membranes, as it is reported to increase membrane fluidity (53, 54). A dose-dependent increase in membrane fluidity on addition of DMSO was observed (Fig. 5B, C). Addition of

5 mM F_3 or F_6 to PC_{100%} or PC_{70%}Cholesterol_{30%} liposomes induced a subtle increase in membrane fluidity (Fig. 5D); however, this increase was less than that expected for the change in membrane fluidity that occurs as a result of a change temperature of 1°C ($3.32 \pm 1.05\%$, Table 2). This parameter was calculated using a previously published dataset (49), where a change in membrane fluidity over a known temperature range for PC-containing liposomes was used to estimate the percentage change in fluidity per 1°C change in temperature from 35°C, not accounting for phase transitions.

Addition of F_3 , but not F_6 , to immortalized neuronal cells induced a dose-dependent reduction in membrane dipole potential without cell toxicity

Incubation of immortalized neuronal cell lines for 24 h with F_3 and F_6 up to concentrations of 10 mM was found to be well-tolerated and cause no significant decline in cell viability versus untreated controls using the AlamarBlue resazurin viability assay (Fig. 6C). The di-8-ANEPPs-labeled immortalized neuronal cells had an average basal membrane dipole potential of 367 ± 6 mV. Addition of F_3 was found to induce a dose-dependent decrease in di-8-ANEPPs fluorescence ratio at 420/520 nm excitation, which fit best to a plateau followed by an exponential decay (Fig. 6A). No detectable change in the di-8-ANEPPs fluorescent ratio was observed on addition of equivalent concentrations of F_6 to cells (Fig. 6B). Plotting the change in terms of membrane dipole potential revealed that addition of F_6 to cells up to concentrations of 5 mM induced no significant change in the membrane dipole potential. In contrast, the addition of F_3 induced a dose-dependent and significant reduction in the dipole potential with a plateau ~ 35 mV (Fig. 6D).

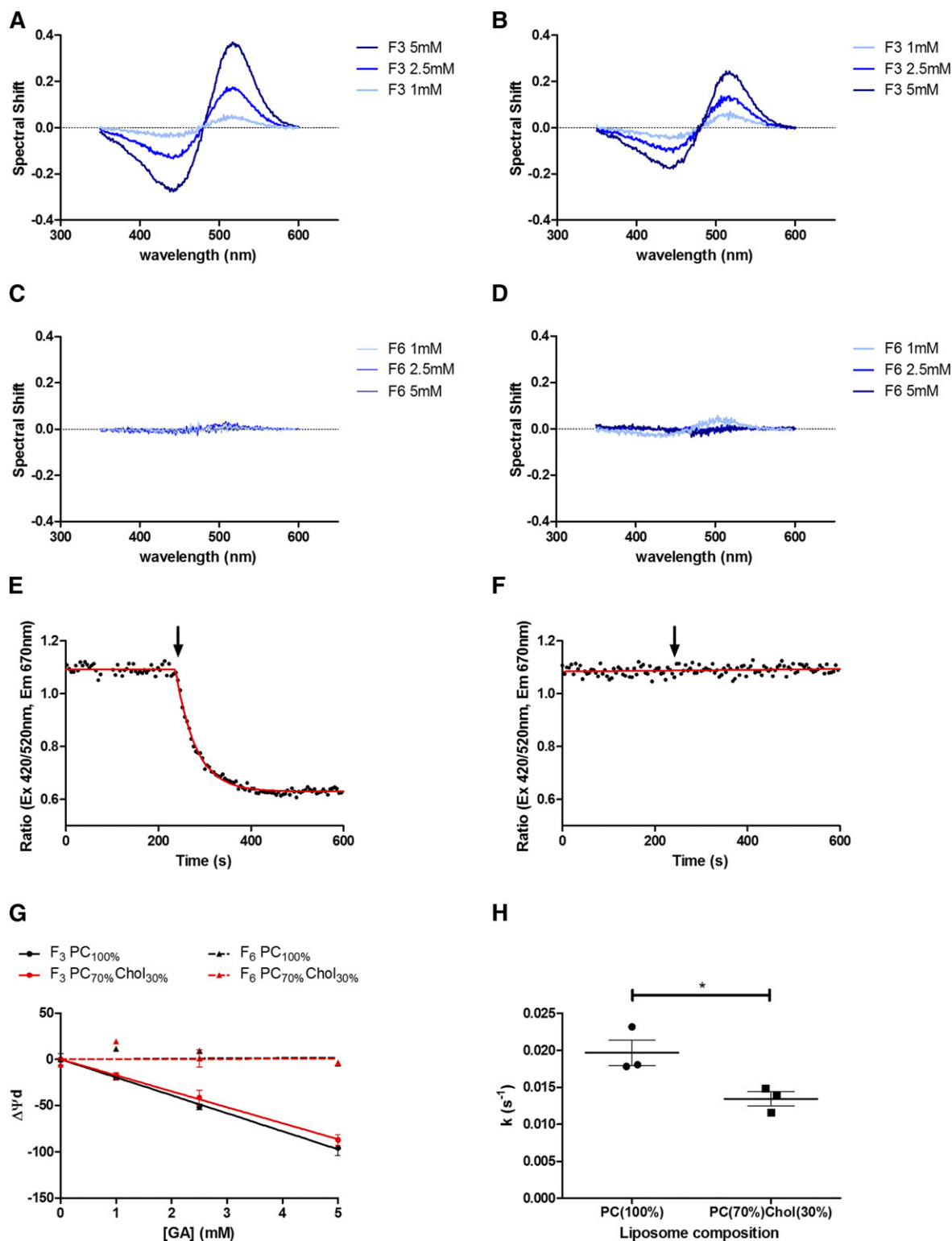


Fig. 3. Comparing the interactions of F₃ and F₆ with artificial membrane systems and their effects on the membrane dipole potential. A–D: The fluorescence excitation spectra of di-8-ANEPPs-labeled liposomes shifts in response to F₃, but not F₆, indicative of a reduction in the membrane dipole potential. Fluorescence difference spectra obtained by subtracting excitation spectra ($\lambda_{em} = 670$ nm) of di-8-ANEPPs-labeled PC_{100%} [PC(100%)] (A, C) and PC_{70%}Cholesterol_{30%} [PC(70%)Chol(30%)] (B, D) liposomes (400 μ M) from those obtained from addition of the indicated concentrations of F₃ (A, B) or F₆ (C, D). Before subtraction, each spectrum was normalized to their integrated areas so that the difference spectra only reflected the spectral shift. In each experiment, temperature was maintained at 37°C. A dual wavelength ratiometric measurement of the membrane dipole potential was made on addition of F₃ (E) or F₆ (F) to di-8-ANEPPs-labeled PC_{100%} liposomes at the indicated time (arrows represent 5 mM additions). Samples were excited at 420 and 520 nm and emission recorded at 670 nm. The ratio R(420/520) was calculated (black dots) before each titration was fit (red line) to a plateau followed by one-phase decay (equation 1) or straight line (equation 2) using an extra sum-of-squares F-test to determine the best fitting model in each case. G: Addition of F₃ (solid

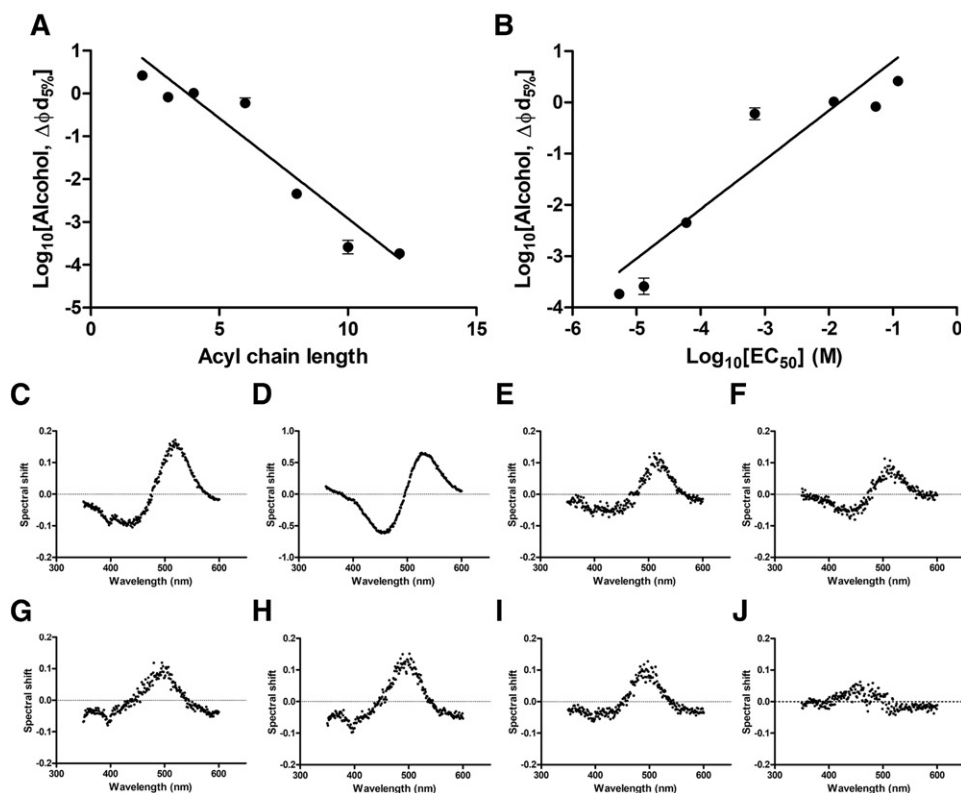


Fig. 4. Comparing the interactions of a series of primary alcohols with artificial membrane systems and their effects on the membrane dipole potential. **A:** The concentration of primary alcohol required to induce a 5% (~ 18 mV) reduction in the membrane dipole potential versus acyl chain length indicates a significant negative correlation (slope = -0.48 ± 0.04 , Spearman's $R = -0.964$, $P = 0.0028$) between acyl chain length and dipole potential modulating effect until tetradodecanol (C14), where a clear cut-off point is observed. **B:** A significant positive correlation (slope = 0.9618 ± 0.09172 , Spearman's $R = 0.964$, $P = 0.0028$) between the effect of primary alcohols on dipole potential modulation and anesthetic potency previously reported in tadpoles (51, 52). **C–J:** The fluorescence excitation spectra of di-8-ANEPPs-labeled liposomes shifts in response to addition of primary alcohols [ethanol (C), propanol (D), butanol (E), hexanol (8.9 mM) (F), octanol (2.7 mM) (G), decanol (0.26 mM) (H), and dodecanol (0.15 mM) (I)] indicative of a reduction in the membrane dipole potential. Fluorescence difference spectra obtained by subtracting excitation spectra ($\lambda_{em} = 670$ nm) of di-8-ANEPPs-labeled PC_{100%} after addition of primary alcohols from baseline values, as previously described in the text. Interestingly, addition of 0.17 mM tetradodecanol to this artificial membrane system caused no such change in the membrane dipole potential (J).

Cholesterol depletion in neuronal cells permits greater anesthetic-mediated dipole potential changes

Depletion of membrane cholesterol content by pretreatment of immortalized neuronal cells with M β CD significantly reduced their membrane dipole potential (295.6 ± 1 mV vs. 367 ± 6 mV, unpaired t -test, $P < 0.0001$) in agreement with previous studies (55). Subsequent application of 5 mM of F₃ to these cells induced a large reduction in the di-8-ANEPPs fluorescence ratio (Fig. 7A), which equated to a significantly greater (two-tailed unpaired t -test, $P = 0.0061$) change in the dipole potential compared with native cells subject to exposure to the same concentration of F₃ (Fig. 7B). The rate of F₃-mediated dipole potential modulation in native cells was significantly greater than that found in cholesterol-depleted cells (0.032 ± 0.01 s⁻¹ vs. 0.01 ± 0.002 s⁻¹, two-tailed unpaired t -test, $P = 0.0122$) (Fig. 7C).

DISCUSSION

This study sought to determine whether the difference in anesthetic activity of the well-described inducer/noninducer pair, F₃ and F₆, could be explained by their ability to differentially modulate the membrane dipole potential. Building on the work of Qin, Szabo, and Cafiso (29), who originally postulated that GA activity may be mediated by modulation of the membrane dipole potential, we sought to investigate this phenomenon using the ratio-metric probe, di-8-ANEPPs, with artificial and cell membrane systems. The first attempt to provide a theory to describe the mechanism of anesthetic action was proposed independently by Meyer and Overton in 1899, who described a correlation between GA potency and oil solubility (56, 57). Since that time, several theories developed that

lines), but not F₆ (dashed lines), to PC_{100%} (black) and PC_{70%}Cholesterol_{30%} (red) artificial membrane systems induced a dose-dependent reduction in the membrane dipole potential. All experiments $n = 3$; mean \pm SEM. **H:** The rate of change in membrane dipole potential on addition of 5 mM F₃ to PC_{100%} liposomes was significantly greater (two-tailed unpaired t -test, $*P = 0.0352$).

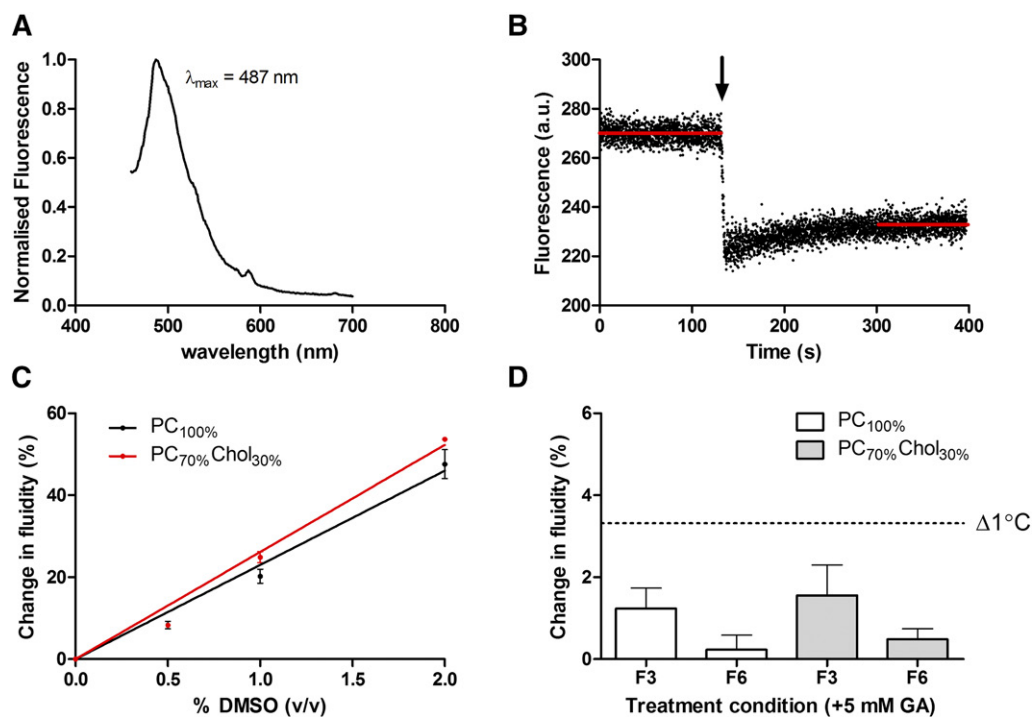


Fig. 5. The influence of F₃ and F₆ on membrane fluidity. **A:** Normalized emission spectra of DCVJ-labeled PC_{100%} liposomes (400 μM liposomes with 1.5 μM dye) in HEPES buffered saline (pH 7.4) at 37°C exhibits peak fluorescence emission of 487 nm, similar to that previously reported for PC liposomes (49). **B:** Addition of 2% DMSO to DCVJ-labeled PC_{100%} liposomes at 37°C induced a reduction in DCVJ fluorescence indicative of an increase in membrane fluidity in agreement with the reported behavior of this molecule in PC- and cholesterol-containing membranes (53, 54). **C:** A concentration-dependent change in membrane fluidity (DCVJ fluorescence intensity ratio) was observed on addition of DMSO to PC_{100%} and PC_{70%}Cholesterol_{30%} [PC_{70%}Chol_{30%}] liposomes at 37°C. On fitting this data to a linear regression model, DMSO was found to induce a significantly greater change in membrane fluidity in PC_{70%}Chol_{30%} membranes, perhaps indicative of disassembly of cholesterol-containing domains (extra sum-of-squares F-test, $P = 0.0246$). **D:** Addition of F₃ and F₆ to liposomes was observed to induce an increase in membrane fluidity with F₃ modulating the membrane fluidity to a greater extent than F₆. The extent of membrane fluidity modulation was, however, slight and less than that typically attributed to a change in temperature of 1°C (Table 2). As mammalian brain temperatures are reported to fluctuate under physiological conditions by up to 3°C (93), this strongly suggests that modulation of membrane fluidity is not responsible for GA action.

postulated mechanisms as to how GAs may exert their effects through membrane interactions, including changes in membrane fluidity (58), volume expansion (59), or surface pressure changes (60). Although these theories provide an attractive explanation as to how GAs with such a diverse family of molecular structures could induce similar effects *in vivo*, over the last three decades several important criticisms have been raised against membrane-mediated theories of GA action. These include: *i*) the observation that small, but physiologically normal, changes in body temperature can induce greater changes in membrane fluidity than those achieved by GA interactions (61, 62); *ii*) the existence of nonanesthetics/nonimmobilizers, a series of molecules whose structure and lipophilicity would suggest GA activity, but do not induce anesthesia (63, 64); *iii*) an unexpected cut-off point in the positive correlation between n-alkane molecular weight and potency despite the oil partition coefficient continuing to increase (1); and *iv*) enantiomers of anesthetic molecules have varying degrees of anesthetic actions, an unexpected result given the achi-rality of the proposed membrane-based mechanisms of action (1).

These criticisms, combined with a seminal study by Franks and Lieb (65) that reported the affinity of GAs for the hydrophobic binding cavity in luciferase also obey the Meyer-Overton relationship, led to a shift in interest more toward protein-based theories of GA action. Since that time, a large number of predominantly protein targets for anesthetics have been identified, including activation of inhibitory ion channels, such as GABA_A, and suppression of excitatory glutamatergic ion channels, such as NMDA receptors (66). Although a wealth of evidence now shows that GAs can modulate ion channel activity and single residue genetic modification of such channels reduces GA potency *in vitro* and *in vivo* (62, 67–69), there are few examples of a clear structure-function relationship between GAs and their ion channel targets (1). Furthermore, given the wide range of potential GA targets, a distinct lack of chemical antagonists, acquired tolerance, and high conservation of potency across the entire animal kingdom suggests that there are likely to be multiple contributing systems to GA activity, rather than a single unitary site of action (70–72). A possible solution to this problem can be found when considering that, in addition to direct ligand-protein interactions,

TABLE 2. The influence of temperature changes on membrane fluidity

Membrane Composition ^a	Technique (Probe) ^a	Temperature (°C) ^a	η (cP) ^a	$\Delta\eta$ (cP)	$\Delta\eta$ (%/°C) ^b
DPPC	Quantum yield (DCVJ)	10–60	120–70	50	1.05
DPPC	Quantum yield (DCQEB)	10–60	30–3	27	3.27
DPPC	fluorescence depolarization (perylene)	25–45	940–94	846	8.18
DPPC	fluorescence depolarization (diphenylhexatriene)	10–60	1,000–50	950	3.62
DPPC	intramolecular excimer formation (dipyrenylpropane)	20–50	30–18	12	1.67
DMPC	Intramolecular excimer formation (dipyrenylpropane)	10–60	125–38	87	2.13
Mean (SE)					3.32 (1.05)

^aDerived from reference (49).

^bNot accounting for phase transitions.

modulation of membrane protein function can also be achieved indirectly by modulating lipid-protein interactions, particularly at the site of membrane rafts (73). For example, both GABA_A and NMDA receptor activity are recognized to be raft associated (74, 75) and their raft distribution is reported to change in response to activation and psychopharmacological challenge (76).

The existence of anesthetic/nonimmobilizer pairs, such as F₃ and F₆, with similar structures and oil partition coefficients, but very different anesthetic activity, has provided both a challenge to determining the processes underlying GA induction and an opportunity to better elucidate their mechanism of action by identifying subtle differences in

behavior. The present study provides evidence to support the theory that modulation of the membrane dipole potential may contribute to the difference in anesthetic activity between the anesthetic/nonanesthetic pair, F₃ and F₆. This study also provides the first evidence to demonstrate GA-mediated modulation of the membrane dipole potential in a living neuronal cell.

Despite their structural similarities and lipophilic nature, F₃ and F₆ possess distinct average dipole moments [3.17 and 0.78 D, respectively (36)] (Fig. 1). As larger dipole moments are reported to impede the penetration of small molecules into biological membranes (77), F₃ would be expected to localize more toward the membrane interface

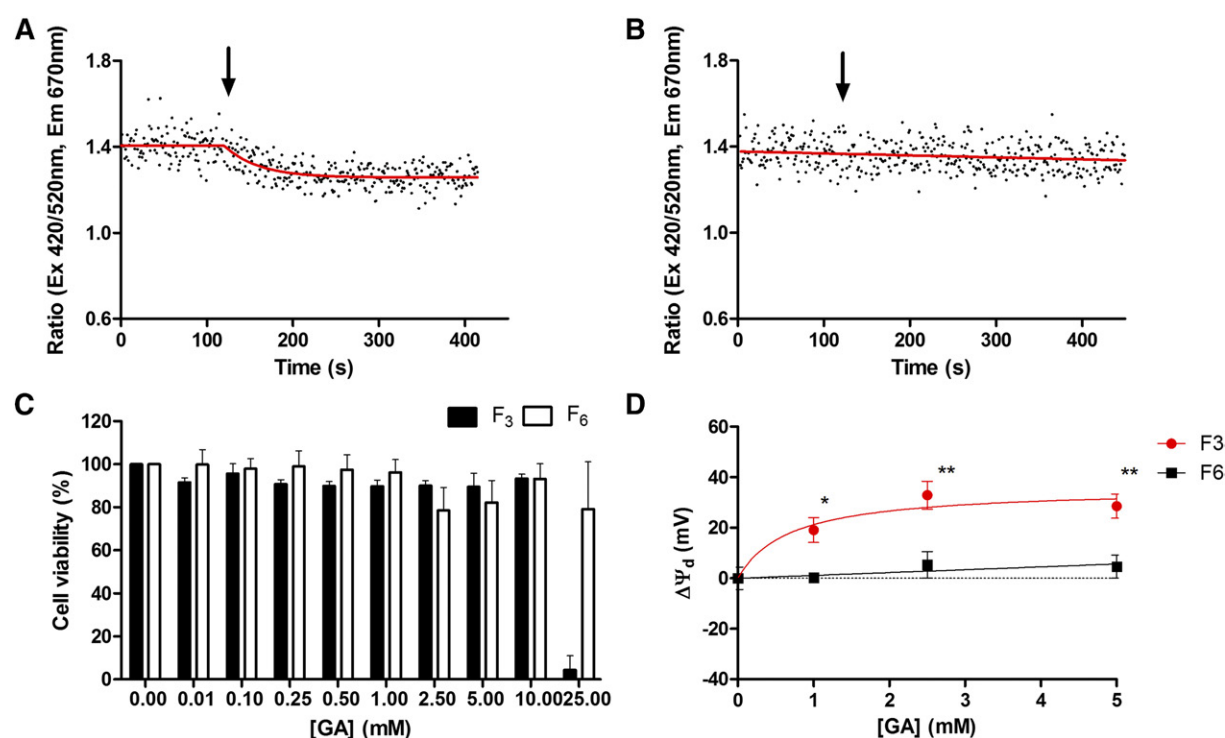


Fig. 6. The interaction of F₃ and F₆ with neuronal cells. Addition (black arrows) of 5 mM F₃ (A), but not 5 mM F₆ (B), induced a reduction in the di-8-ANEPPs fluorescence ratio indicative of a reduction in the membrane dipole potential. C: Immortalized neuronal cell cultures were incubated in the presence of varying concentration of F₃ or F₆ for 24 h before cell viability was assessed using an AlamarBlue assay. No significant change in cell viability was observed on addition of up to 10 mM concentrations of either agent. D: The change in membrane dipole potential induced on addition of F₃ or F₆ to immortalized neuronal cells labeled with di-8-ANEPPs. Profiles were fit to a simple hyperbolic equation or straight line and the best fitting model determined by F-test, $n > 3$, mean \pm SEM.

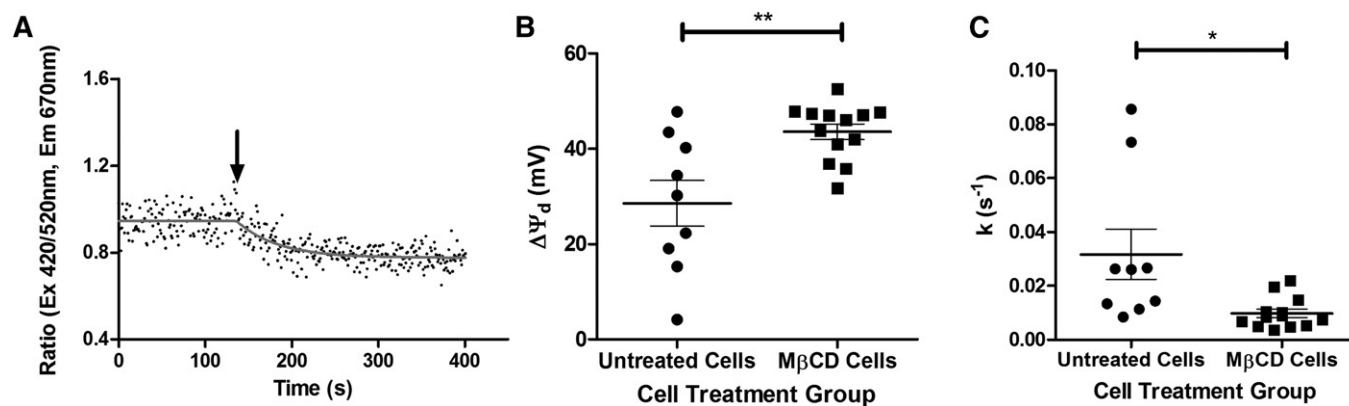


Fig. 7. Depletion of cholesterol using $M\beta CD$ in neuronal cells leads to larger changes in the dipole potential. Example experiment of ratiometric imaging (simultaneous 420/520 nm scans) of $M\beta CD$ -treated cells treated with 5 mM F_3 (A) (arrow represents the addition of F_3). Depletion of cholesterol caused a significantly greater change in the span (B) and rate (C) of the decrease in dipole potential following 5 mM F_3 in ratiometric titration experiments (** $P=0.0028$ and * $P=0.0122$, respectively).

compared with F_6 , which would instead be found more toward the hydrophobic membrane interior. The membrane dipole potential is, itself, comprised of the electrical dipoles associated with the carbonyl group and oxygen-bonded phosphate components of the membrane surface in conjunction with the permanent molecular dipoles of water molecules occupying a restricted conformation in the membrane solvation shell at this site (78–81). The localization of F_3 at the membrane interface would, therefore, be expected to more strongly influence the membrane dipole potential than its nonimmobilizer counterpart, F_6 .

Experimental evidence to support the difference in membrane distribution of F_3 and F_6 was presented in two studies by North and Cafiso (82) and Tang, Yan, and Xu (83), who used 2H and ^{19}F NMR to report that, while F_3 preferentially localizes to the membrane interface, F_6 localizes to the hydrophobic core of the membrane. Interestingly, the authors also reported that halothane, isoflurane, and enflurane also localized at the membrane interface, perhaps suggesting a shared mechanism of action between these molecules. These observations were supported by subsequent studies by Tang et al. (84) and Tang, Simplaceanu, and Xu (85), who used NMR to confirm the site of the water-lipid-protein interface as the site of F_3 interaction with gramicidin A channels. More recently, Bondarenko et al. (86) reported that using 1H and ^{15}N solution-state NMR to show that addition of millimolar concentrations of F_3 and isoflurane to nAChR- $\beta 2$ subunit-loaded dodecyl phosphocholine micelles resulted in a change in α -helix conformation through shortening and lengthening of helix hydrogen bonds. Furthermore, the “unsaturable” nature of some of these chemical shifts at high GA concentrations suggests a nonspecific mechanism of action. This work is in agreement with recent observations suggesting that micelles also possess a dipole potential (87) and previous work demonstrating that modulation of membrane dipole potential can induce changes in membrane peptide conformation (80). Based on this data, the difference in average dipole moment leading to the distinct membrane localization of F_3 and F_6 could offer an

attractive mechanism to explain the difference in the ability of these molecules to modulate the membrane dipole potential.

To further test the hypothesis that modulation of membrane dipole potential may provide a potential mechanism of anesthetic action, a series of primary alcohols, which were previously reported to have anesthetic effects (51), were titrated into artificial membranes and the change in dipole potential recorded. A significant negative correlation between acyl chain length and ability to modulate the membrane dipole potential was observed. The concentration of primary alcohol required to induce a 5% change in the membrane dipole potential of $PC_{100\%}$ liposomes (~ 18 mV) was found to strongly correlate with the reported EC_{50} of each molecule, including a cut-off in dipole potential modulation at C14 (tetradodecanol) (51), despite reports that primary alcohols continue to partition into lipid bilayers with increasing chain length up to 15 carbons in length (88) and no qualitative difference in the ability of the anesthetic alcohol, dodecanol, and nonanesthetic alcohol, tetradodecanol, to achieve effective levels in tadpoles, suggesting that this cut-off is not due to the reducing solubility of longer chain alcohols (89). This observation is in agreement with previous work by Ingolfsson and Anderson (90), who reported that the presence of such alcohol cut-offs can exist in the absence of a specific alcohol binding site within the system (i.e., an alcohol binding protein), supportive of indirect modulation of membrane properties as a mechanism of anesthesia induction.

Previous membrane-based explanations for the cut-off point between dodecanol and tetradodecanol include the observation by Chiou et al. (91), who, using FTIR, found that hydrogen bond breaking activity of the primary alcohol series at the membrane-water interface correlates with anesthetic potency and includes a marked cut-off point between 10 and 14 carbons. A similar hydrogen-bond breaking propensity for fluorocarbon anesthetics had previously been reported by Di Paolo and Sandorfy (92); although in both cases, the process linking interfacial hydrogen-bond breaking and anesthesia induction remained elusive.

As previously described, the membrane dipole potential is comprised of the electrical dipoles associated with the carbonyl group and oxygen-bonded phosphate components of the membrane surface in conjunction with the permanent molecular dipoles of water molecules occupying a restricted conformation in the membrane solvation shell at this site (78–81). Together, these observations suggest that anesthetic-induced disruption of lipid-water hydrogen bonds at the membrane-water interface could explain the changes in the membrane dipole potential induced by F_3 and primary alcohols up to dodecanol, but not tetradodecanol.

Although independent of the membrane dipole potential (22), modulation of membrane fluidity has been postulated as an alternative mechanism of anesthetic action (58). Using DCVJ, a small increase in membrane fluidity was observed on addition of F_3 and F_6 to PC_{100%} and PC_{70%}Cholesterol_{30%} liposomes and the change in fluidity induced by F_3 was found to be greater than F_6 (although this difference was not significant). The change in fluidity was, however, found to be less than that induced by a 1°C temperature change (Table 2), in agreement with previous observations for other GA/membrane interactions (61, 62). This result strongly suggests that changes in membrane fluidity are, therefore, not responsible for GA activity, as the temperature of the mammalian brain is reported to fluctuate by up to 3°C under physiological conditions (93).

The addition of DMSO to DCVJ-labeled PC_{100%} and PC_{70%}Cholesterol_{30%} liposomes (Fig. 5B, C) was found to induce a relatively large dose-dependent increase in membrane fluidity, despite DMSO possessing no anesthetic activity (94). A significantly greater change in membrane fluidity was observed on addition of DMSO to PC_{70%}Cholesterol_{30%} membranes (slope: $23.0 \pm 1.1\%$ vs. $26.1 \pm 0.7\%$ $\Delta\eta/1\%$ (v/v) DMSO, extra sum-of-squares F-test, $P = 0.0246$). The marked change in membrane fluidity in response to these relatively low concentrations of DMSO may offer a novel mechanism for the recently reported toxicity of <2% concentrations of DMSO in vitro and in vivo (95), recognizing a potential link between membrane fluidity and apoptosis induction (96).

This study provides the first evidence to suggest that addition of F_3 (but not F_6) to immortalized neuronal cells can induce a dose-dependent reduction in membrane dipole potential equivalent to -19.1 ± 4.5 mV at 1 MAC equivalent without negatively impacting cell viability. Immortalized cell lines provide an attractive model for this work, owing to the clonal nature of the cells and the large number required for these experiments, which precluded isolation from primary tissues. A limitation of working with immortalized cells, however, is that they serve only as a model of retinal neuron cell behavior, which may not reflect the behavior of cells in vivo.

While it is extremely difficult to extrapolate clinically relevant anesthetic concentration for in vitro studies from parameters such as MAC (71), several studies have assessed the concentrations of F_3 required to modulate the function of proteins linked to GA activity in vitro. The majority of these studies were conducted by examining the effect of GAs using two-electrode voltage clamp recording in

Xenopus oocytes expressing membrane proteins with suspected GA activity. Low millimolar concentrations of F_3 (typically 0.2–5 mM), but not F_6 , were reported to strongly potentiate the action of glycine on homomeric α -glycine receptor subunits in a concentration-dependent manner (97); inhibit muscarinic m_1 receptor-induced Ca²⁺-dependent chloride currents (98); inhibit a number of potassium channels, including ERG-1, KCNQ2/3, and GIRK (99); and inhibit synaptosomal sodium channels (38, 100) and NMDA receptors (68). Beyond this model, Liachenko et al. (101) investigated the effects of clinically relevant concentrations (2 MAC) of F_3 and F_6 on K⁺-evoked glutamate and GABA release from isolated and superfused cerebrocortical slices from mice. F_3 (1.6 ± 0.11 mM), but not F_6 , was reported to suppress evoked glutamate release by 70%, but had no significant effects on evoked GABA release, without causing any nonspecific or irreversible changes in the brain slices. In summary, the concentrations of F_3 reported modulating the membrane dipole potential in both artificial and neuronal membrane systems closely match those reported to modulate a range of membrane protein functions in other models.

The incorporation of 30% molar cholesterol into PC liposomes was found to reduce both the magnitude and rate of change in dipole potential on addition of F_3 . In agreement with this observation, depletion of cholesterol from neuronal cell membranes with M β CD was found to increase the change in membrane dipole potential on addition of F_3 by almost 50%. Surprisingly, the rate of dipole potential change on depletion of membrane cholesterol was found to decrease. This may be indicative of the influence of other membrane components (i.e., charged lipids or sphingomyelin) on the interactions of F_3 with the membrane or be a result of the recognized limitations of M β CD-mediated cholesterol depletion (102). These observations are in agreement with previous work that reported that cholesterol can inhibit the pentobarbital-mediated suppression of human brain sodium channels in planar lipid bilayers in a concentration-dependent manner (103). A possible mechanism for this process is the exclusion of F_3 from cholesterol-containing membrane microdomains (rafts) (104), dynamic structures that may offer an additional level of control over membrane protein function. Future work will seek to isolate raft and nonraft domains from immortalized retinal neuronal cells in order to quantitatively determine the distribution of F_3 and F_6 between these distinct membrane domains.

A membrane dipole potential-mediated mechanism of anesthesia action can also offer an explanation why enantiomers of anesthetic molecules can possess different activities. An often overlooked, but important, property of biological membranes is that they also possess chirality. For example, PC possesses a chiral center at the position of the C2 carbon of the glycerol backbone and the plasma membrane comprises L-optical isomers of PC (105). With the growing recognition that enantioselective interactions between membrane constituents can determine the physical properties of membranes (106), including the formation and organization of membrane rafts (107), it is an intriguing

hypothesis that enantiomeric anesthetics, interacting at the membrane interface at the site of the membrane dipole potential, may elicit varying degrees of activity without requiring direct protein interactions. Support for this view can be found in recent work by Bandari et al. (24), who present intriguing evidence to suggest that the membrane dipole potential is sensitive to the stereospecificity of cholesterol, which can significantly alter the dipolar field at the membrane interface that can, in turn, modulate membrane protein activity.

Confocal scanning laser ophthalmoscopy is an established technique for noninvasive retinal visualization that is increasingly being combined with fluorescent contrast agents to increase the amount of information that can be extracted for retinal imaging purposes. For example, fluorescein and indocyanine green angiography permits diagnosis of retinal disorders via visualization of retinal and choroidal vasculature abnormalities (108) and, more recently, our group has developed the DARC (detection of apoptotic retinal cell) technology that uses fluorescently labeled annexin A5 to provide a snapshot of the number of dying cells in the retina at a specific time point (109, 110). Assuming modulation of membrane dipole potential is a common feature among other GA molecules, the ratiometric probe, di-8-ANEPPs, could provide a useful tool to monitor changes in the membrane dipole potential in response to GA induction using retinal imaging approaches. Future work will seek to establish whether modulation of membrane dipole potential can

be used to predict anesthetic sensitivity for a broad range of anesthetic species and develop both a noninvasive administration technique of the di-8-ANEPPs contrast agent in rodent models and a ratiometric fluorescence-based imaging device for the real-time screening of patients' responses to anesthesia in a preoperative environment. We anticipate that patients susceptible to AAGA will exhibit a reduced modulation in the membrane dipole potential in response to administration of subclinical doses of GAs, which could be easily monitored by noninvasive ophthalmic examination using ratiometric confocal scanning laser ophthalmoscopy, such as the device outlined in Fig. 8.

As AAGA may be the result of a number of factors, including failure to deliver or maintain sufficient GA in the CNS [perhaps due to differences in the activity of protein transporters or drug metabolism (111)], the authors postulate that AAGA-associated changes in GA sensitivity could manifest as: *i*) a difference in the onset of CNS dipole potential modulation after GA administration; *ii*) the magnitude of the resulting dipole potential change; or *iii*) a reduction in the duration of the changed dipole potential state after administration of a fixed subclinical dose of GA. This hypothesis assumes that there exists a strong association between the changes in membrane dipole in the CNS and GA activity in anesthetics in addition to F₃, enflurane, isoflurane, and halothane, described previously (29), and that retinal response to GA induction mirrors changes in the rest of the CNS.

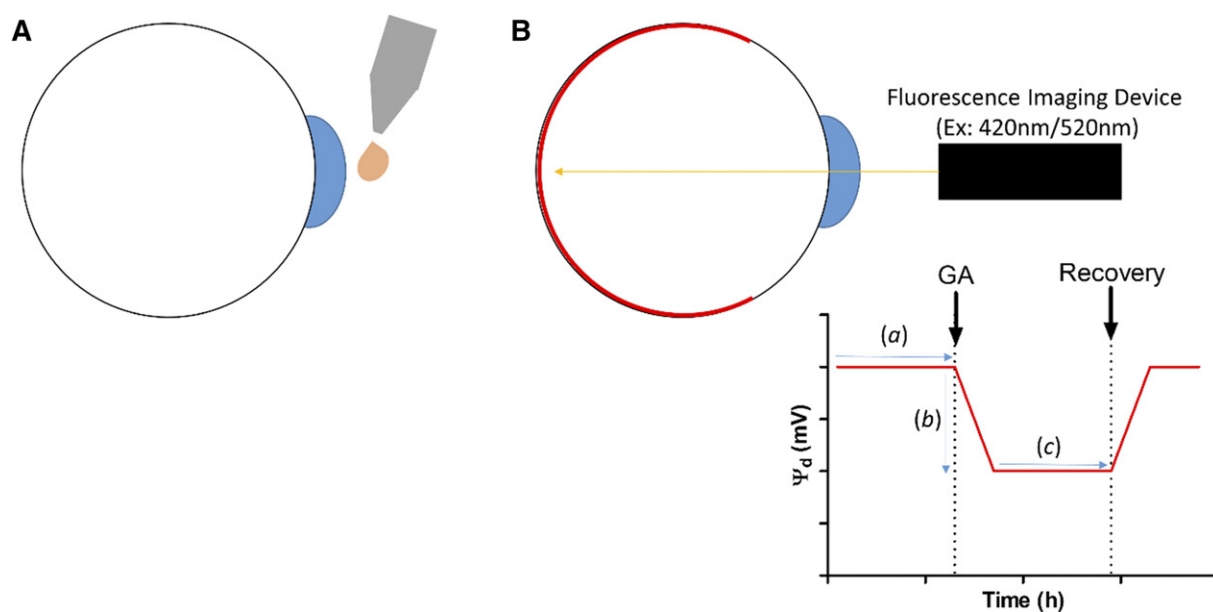



Fig. 8. A proposed schematic of a confocal scanning laser ophthalmoscopy-based technique for monitoring GA susceptibility using di-8-ANEPPs-mediated ratiometric real-time monitoring of the membrane dipole potential. A: The di-8-ANEPPs contrast agent will be administered locally (topically) prior to surgery to permit retinal membrane dipole potential values to be recorded before administration of subclinical doses of GA. B: After GA administration, real-time depth of GA monitoring could be achieved by recording the di-8-ANEPPs fluorescent ratio; as the retina is part of the CNS, we anticipate that changes in the retinal membrane dipole potential recorded in this tissue will mirror changes reported in the brain in response to GA. These changes could present as differences in the onset of CNS dipole potential modulation after GA administration (*a*), the magnitude of the resulting dipole potential change (*b*), or a reduction in the duration of the changed dipole potential state after administration of a fixed subclinical dose of GA (*c*). Changes could manifest as a result of systemic differences in GA delivery to the CNS (i.e., changes in multidrug efflux pump activity or GA metabolism) and not necessarily simply changes in CNS membrane composition in individuals susceptible to AAGA.

In summary, this work supports previous observations that suggest that modulation of the membrane dipole potential could provide a mechanism to explain the difference in anesthetic action of the inducer/noninducer pair, F₃ and F₆, and the existence of a cut-off in anesthetic activity in the primary alcohol series. An advantage of this membrane-mediated mechanism of GA action is that it may address some of the limitations of existing membrane-mediated hypotheses, including the existence of nonimmobilizers and perhaps even stereospecificity (24). Assuming that other GAs behave in a similar manner to those outlined here and in previous work (29), we anticipate that the process of dipole potential-mediated GA action will manifest via indirect modulation of membrane protein function, such as the type II interactions recently described by Richens et al. (73). We propose the use of di-8-ANEPPs-mediated reporting of the membrane dipole potential as a technique to preoperatively screen patients for anesthetic susceptibility and risk of AAGA by combining this probe with confocal scanning laser ophthalmoscopy. 

The authors are grateful to Professor Paul O'Shea (University of Nottingham) for useful discussion.

REFERENCES

- Kopp Lugli, A., C. S. Yost, and C. H. Kindler. 2009. Anaesthetic mechanisms: update on the challenge of unravelling the mystery of anaesthesia. *Eur. J. Anaesthesiol.* **26**: 807–820.
- Rosenberg, H., N. Pollock, A. Schiemann, T. Bulger, and K. Stowell. 2015. Malignant hyperthermia: a review. *Orphanet J. Rare Dis.* **10**: 93.
- Wichmann, S., G. Færk, J. R. Bundgaard, and M. R. Gätke. 2016. Patients with prolonged effect of succinylcholine or mivacurium had novel mutations in the butyrylcholinesterase gene. *Pharmacogenet. Genomics.* **26**: 351–356.
- Mills, A. T., P. J. Sice, and S. M. Ford. 2014. Anaesthesia-related anaphylaxis: investigation and follow-up. *Contin. Educ. Anaesth. Crit. Care Pain.* **14**: 57–62.
- Messina, A. G., M. Wang, M. J. Ward, C. C. Wilker, B. B. Smith, D. P. Vezina, and N. L. Pace. 2016. Anaesthetic interventions for prevention of awareness during surgery. *Cochrane Database Syst. Rev.* **10**: CD007272.
- Heyse, B., B. Van Ooteghem, B. Wyler, M. M. R. F. Struys, L. Herregods, and H. Vereecke. 2009. Comparison of contemporary EEG derived depth of anesthesia monitors with a 5 step validation process. *Acta Anaesthesiol. Belg.* **60**: 19–33.
- Bainbridge, D., J. Martin, M. Arango, and D. Cheng; Evidence-based Peri-operative Clinical Outcomes Research (EPiCOR) Group. 2012. Perioperative and anaesthetic-related mortality in developed and developing countries: a systematic review and meta-analysis. *Lancet.* **380**: 1075–1081.
- Musizza, B., and S. Ribaric. 2010. Monitoring the depth of anaesthesia. *Sensors (Basel).* **10**: 10896–10935.
- Goddard, N., and D. Smith. 2013. Unintended awareness and monitoring of depth of anaesthesia. *Contin. Educ. Anaesth. Crit. Care Pain.* **13**: 213–217.
- Sury, M. R. J. 2016. Accidental awareness during anesthesia in children. *Pediatr. Anesth.* **26**: 468–474.
- Cook, T. M., J. Andrade, D. G. Bogod, J. M. Hitchman, W. R. Jonker, N. Lucas, J. H. Mackay, A. F. Nimmo, K. O'Connor, E. P. O'Sullivan, et al.; Royal College of Anaesthetists; Association of Anaesthetists of Great Britain and Ireland. 2014. The 5th National Audit Project (NAP5) on accidental awareness during general anaesthesia: patient experiences, human factors, sedation, consent and medicolegal issues. *Anaesthesia.* **69**: 1102–1116.
- Avidan, M. S., and J. W. Sleigh. 2014. Beware the Boojum: the NAP5 audit of accidental awareness during intended general anaesthesia. *Anaesthesia.* **69**: 1065–1068.
- Pandit, J. J., J. Andrade, D. G. Bogod, J. M. Hitchman, W. R. Jonker, N. Lucas, J. H. Mackay, A. F. Nimmo, K. O'Connor, E. P. O'Sullivan, et al.; Royal College of Anaesthetists; Association of Anaesthetists of Great Britain and Ireland. 2014. 5th National Audit Project (NAP5) on accidental awareness during general anaesthesia: summary of main findings and risk factors. *Br. J. Anaesth.* **113**: 549–559.
- Domino, K. B., K. L. Posner, R. A. Caplan, and F. W. Cheney. 1999. Awareness during anesthesia: a closed claims analysis. *Anesthesiology.* **90**: 1053–1061.
- Ghoneim, M. M., R. I. Block, M. Haffarman, and M. J. Mathews. 2009. Awareness during anesthesia: risk factors, causes and sequelae: a review of reported cases in the literature. *Anesth. Analg.* **108**: 527–535.
- Aranake, A., S. Gradwohl, A. Ben-Abdallah, N. Lin, A. Shanks, D. L. Helsten, D. B. Glick, E. Jacobsohn, A. J. Villafranca, A. S. Evers, et al. 2013. Increased risk of intraoperative awareness in patients with a history of awareness. *Anesthesiology.* **119**: 1275–1283.
- Checketts, M. R., R. Alladi, K. Ferguson, L. Gemmell, J. M. Handy, A. A. Klein, N. J. Love, U. Misra, C. Morris, M. H. Nathanson, et al.; Association of Anaesthetists of Great Britain and Ireland. 2015. Recommendations for standards of monitoring during anaesthesia and recovery 2015: Association of Anaesthetists of Great Britain and Ireland. *Anaesthesia.* **71**: 85–93.
- Li, T.-N., and Y. Li. 2014. Depth of anaesthesia monitors and the latest algorithms. *Asian Pac. J. Trop. Med.* **7**: 429–437.
- Yli-Hankala, A., and H. Scheinin. 2015. [Is it possible to measure the depth of anesthesia using electroencephalogram?]. *Duodecim.* **131**: 1929–1936. Finnish.
- O'Shea, P. 2005. Physical landscapes in biological membranes: physico-chemical terrains for spatio-temporal control of biomolecular interactions and behaviour. *Philos. Trans. A Math. Phys. Eng. Sci.* **363**: 575–588.
- Yang, Y., K. M. Mayer, N. S. Wickremasinghe, and J. H. Hafner. 2008. Probing the lipid membrane dipole potential by atomic force microscopy. *Biophys. J.* **95**: 5193–5199.
- Clarke, R. J., and D. J. Kane. 1997. Optical detection of membrane dipole potential: avoidance of fluidity and dye-induced effects. *Biochim. Biophys. Acta.* **1323**: 223–239.
- Starke-Peterkovic, T., N. Turner, M. F. Vitha, M. P. Waller, D. E. Hibbs, and R. J. Clarke. 2006. Cholesterol effect on the dipole potential of lipid membranes. *Biophys. J.* **90**: 4060–4070.
- Bandari, S., H. Chakraborty, D. F. Covey, and A. Chattopadhyay. 2014. Membrane dipole potential is sensitive to cholesterol stereospecificity: implications for receptor function. *Chem. Phys. Lipids.* **184**: 25–29.
- Sharom, F. J. 2014. Complex interplay between the P-glycoprotein multidrug efflux pump and the membrane: its role in modulating protein function. *Front. Oncol.* **4**: 41.
- Davis, S., B. M. Davis, J. L. Richens, K. Vere, P. G. Petrov, C. P. Winlove, and P. O. Shea. 2015. α -Tocopherols modify the membrane dipole potential leading to modulation of ligand binding by P-glycoprotein. *J. Lipid Res.* **56**: 1543–1550.
- Davis, B. M., R. Jensen, P. Williams, and P. O'Shea. 2010. The interaction of N-acylhomoserine lactone quorum sensing signaling molecules with biological membranes: implications for inter-kingdom signaling. *PLoS One.* **5**: e13522.
- Asawakarn, T., J. Cladera, and P. O'Shea. 2001. Effects of the membrane dipole potential on the interaction of saquinavir with phospholipid membranes and plasma membrane receptors of Caco-2 cells. *J. Biol. Chem.* **276**: 38457–38463.
- Qin, Z., G. Szabo, and D. S. Cafiso. 1995. Anesthetics reduce the magnitude of the membrane dipole potential. Measurements in lipid vesicles using voltage-sensitive spin probes. *Biochemistry.* **34**: 5536–5543.
- Rokitskaya, T. I., E. A. Kotova, and Y. N. Antonenko. 2002. Membrane dipole potential modulates proton conductance through gramicidin channel: movement of negative ionic defects inside the channel. *Biophys. J.* **82**: 865–873.
- Efimova, S. S., A. A. Zakharova, L. V. Schagina, and O. S. Ostroumova. 2016. Local anesthetics affect gramicidin A channels via membrane electrostatic potentials. *J. Membr. Biol.* **249**: 781–787.

32. Starke-Peterkovic, T., N. Turner, P. L. Else, and R. J. Clarke. 2005. Electric field strength of membrane lipids from vertebrate species: membrane lipid composition and Na⁺-K⁺-ATPase molecular activity. *Am. J. Physiol. Regul. Integr. Comp. Physiol.* **288**: R663–R670.
33. Davis, B. M., L. Crawley, M. Pahlitzsch, F. Javaid, and M. F. Cordeiro. 2016. Glaucoma: the retina and beyond. *Acta Neuropathol.* **132**: 807–826.
34. Lalonde, M. R., B. C. Chauhan, and F. Tremblay. 2006. Retinal ganglion cell activity from the multifocal electroretinogram in pig: optic nerve section, anaesthesia and intravitreal tetrodotoxin. *J. Physiol.* **570**: 325–338.
35. Gross, E., R. S. Bedlack, and L. M. Loew. 1994. Dual-wavelength ratiometric fluorescence measurement of the membrane dipole potential. *Biophys. J.* **67**: 208–216.
36. Saladino, A. C., and P. Tang. 2004. Optimization of structures and LJ parameters of 1-chloro-1,2,2-trifluorocyclobutane and 1,2-dichlorohexafluorocyclobutane. *J. Phys. Chem. A.* **108**: 10560–10564.
37. Koblin, D. D., B. S. Chortkoff, M. J. Laster, E. I. Eger II, M. J. Halsey, and P. Inescu. 1994. Polyhalogenated and perfluorinated compounds that disobey the Meyer-Overton hypothesis. *Anesth. Analg.* **79**: 1043–1048.
38. Ratnakumari, L., T. N. Vysotskaya, D. S. Duch, and H. C. Hemmings, Jr. 2000. Differential effects of anesthetic and non-anesthetic cyclobutanes on neuronal voltage-gated sodium channels. *Anesthesiology*. **92**: 529–541.
39. Mihic, S. J., Q. Ye, M. J. Wick, V. V. Koltchine, M. D. Krasowski, S. E. Finn, M. P. Mascia, C. F. Valenzuela, K. K. Hanson, E. P. Greenblatt, et al. 1997. Sites of alcohol and volatile anaesthetic action on GABA(A) and glycine receptors. *Nature*. **389**: 385–389.
40. Jewell, S. A., P. G. Petrov, and C. P. Winlove. 2013. The effect of oxidative stress on the membrane dipole potential of human red blood cells. *Biochim. Biophys. Acta.* **1828**: 1250–1258.
41. Chen, Y., and R. J. Rivers. 2001. Measurement of membrane potential and intracellular Ca(2+) of arteriolar endothelium and smooth muscle in vivo. *Microvasc. Res.* **62**: 55–62.
42. Mayer, L. D., M. J. Hope, and P. R. Cullis. 1986. Vesicles of variable sizes produced by a rapid extrusion procedure. *Biochim. Biophys. Acta.* **858**: 161–168.
43. Krishnamoorthy, R. R., P. Agarwal, G. Prasanna, K. Vopat, W. Lambert, H. J. Sheedlo, I. H. Pang, D. Shade, R. J. Wordinger, T. Yorio, et al. 2001. Characterization of a transformed rat retinal ganglion cell line. *Brain Res. Mol. Brain Res.* **86**: 1–12.
44. Burugula, B., B. S. Ganesh, and S. K. Chintala. 2011. Curcumin attenuates staurosporine-mediated death of retinal ganglion cells. *Invest. Ophthalmol. Vis. Sci.* **52**: 4263–4273.
45. Nadal-Nicolás, F. M., M. Jiménez-López, P. Sobrado-Calvo, L. Nieto-López, I. Cánovas-Martínez, M. Salinas-Navarro, M. Vidal-Sanz, and M. Agudo. 2009. Brn3a as a marker of retinal ganglion cells: qualitative and quantitative time course studies in naive and optic nerve-injured retinas. *Invest. Ophthalmol. Vis. Sci.* **50**: 3860–3868.
46. Al-Ubaidi, M. R. 2014. RGC-5: are they really 661W? The saga continues. *Exp. Eye Res.* **119**: 115.
47. Van Bergen, N. J., J. P. Wood, G. Chidlow, I. A. Trounce, R. J. Casson, W. K. Ju, R. N. Weinreb, and J. G. Crowston. 2009. Recharacterization of the RGC-5 retinal ganglion cell line. *Invest. Ophthalmol. Vis. Sci.* **50**: 4267–4272.
48. Krishnamoorthy, R. R., A. F. Clark, D. Daudt, J. K. Vishwanatha, and T. Yorio. 2013. A forensic path to RGC-5 cell line identification: lessons learned. *Invest. Ophthalmol. Vis. Sci.* **54**: 5712–5719.
49. Kung, C. E., and J. K. Reed. 1986. Microviscosity measurements of phospholipid bilayers using fluorescent dyes that undergo torsional relaxation. *Biochemistry*. **25**: 6114–6121.
50. Haidekker, M. A., T. Ling, M. Anglo, H. Y. Stevens, J. A. Frangos, and E. A. Theodorakis. 2001. New fluorescent probes for the measurement of cell membrane viscosity. *Chem. Biol.* **8**: 123–131.
51. Pringle, M. J., K. B. Brown, K. W. Miller, S. Pringle, and K. B. Brown. 1980. Can the lipid theories of anesthesia account for the cutoff in anesthetic potency in homologous series of alcohols? *Mol. Pharmacol.* **19**: 49–55.
52. Alifimoff, J. K., L. L. Firestone, and K. W. Miller. 1989. Anaesthetic potencies of primary alkanols: implications for the molecular dimensions of the anaesthetic site. *Br. J. Pharmacol.* **96**: 9–16.
53. Chang, H. H., and P. K. Dea. 2001. Insights into the dynamics of DMSO in phosphatidylcholine bilayers. *Biophys. Chem.* **94**: 33–40.
54. de Ménorval, M-A., L. M. Mir, M. L. Fernández, and R. Reigada. 2012. Effects of dimethyl sulfoxide in cholesterol-containing lipid membranes: a comparative study of experiments in silico and with cells. *PLoS One*. **7**: e41733.
55. Starke-Peterkovic, T., N. Turner, M. F. Vitha, M. P. Waller, D. E. Hibbs, and R. J. Clarke. 2006. Cholesterol effect on the dipole potential of lipid membranes. *Biophys. J.* **90**: 4060–4070.
56. Overton, E. 1899. Ueber die allgemeinen osmotischen Eigenschaften der Zelle, ihre vermutlichen Ursachen und ihre Bedeutung für die Physiologie. *Vierteljahrsschr. Naturforsch. Ges. Zürich.* **44**: 88–135.
57. Meyer, H. H. 1899. Welche Eigenschaft der Anästhetika bedingt ihre narkotische Wirkung? *Arch. Exp. Pathol. Pharmacol. (Naunyn-Schmiedeberg's)*. **42**: 109–118.
58. Ueda, I., M. Hirakawa, K. Arakawa, and H. Kamaya. 1986. Do anaesthetics fluidize membranes? *Anesthesiology*. **64**: 67–71.
59. Mori, T., N. Matubayasi, and I. Ueda. 1984. Membrane expansion and inhalation anaesthetics. Mean excess volume hypothesis. *Mol. Pharmacol.* **25**: 123–130.
60. Cantor, R. S. 1997. The lateral pressure profile in membranes: a physical mechanism of general anaesthesia. *Biochemistry*. **36**: 2339–2344.
61. Eger, E. I., B. Saidman, and L. Brandstater. 1965. Temperature dependence of halothane and cyclopropane anaesthesia in dogs: correlation with some theories of anaesthetic action. *Anesthesiology*. **26**: 764–770.
62. Weir, C. J. 2006. The molecular mechanisms of general anaesthesia: dissecting the GABA A receptor. *Contin. Educ. Anaesth. Crit. Care Pain.* **6**: 49–53.
63. Sonner, J. M., J. Li, and E. I. Eger. 1998. Desflurane and the non-immobilizer 1,2-dichlorohexafluorocyclobutane suppress learning by a mechanism independent of the level of unconditioned stimulation. *Anesth. Analg.* **87**: 200–205.
64. Kandel, L., B. Chortkoff, J. Sonner, M. Laster, and D. Eger. 1996. Nonanesthetics can suppress learning. *Anesth. Analg.* **82**: 321–326.
65. Franks, N. P., and W. Lieb. 1984. Do general anaesthetics act by competitive binding to specific receptors? *Nature*. **310**: 599–601.
66. Dilger, J. P. 2002. The effects of general anaesthetics on ligand-gated ion channels. *Br. J. Anaesth.* **89**: 41–51.
67. Minami, K., M. J. Wick, Y. Stern-Bach, J. E. Dildy-Mayfield, S. J. Brozowski, E. L. Gonzales, J. R. Trudell, and R. A. Harris. 1998. Sites of volatile anaesthetic action on kainate (glutamate receptor 6) receptors. *J. Biol. Chem.* **273**: 8248–8255.
68. Ogata, J., M. Shiraishi, T. Namba, C. T. Smothers, J. J. Woodward, and R. A. Harris. 2006. Effects of anaesthetics on mutant N-methyl-D-aspartate receptors expressed in *Xenopus* oocytes. *J. Pharmacol. Exp. Ther.* **318**: 434–443.
69. Franks, N. P. 2008. General anaesthesia: from molecular targets to neuronal pathways of sleep and arousal. *Nat. Rev. Neurosci.* **9**: 370–386.
70. Eckenhoff, M. F., K. Chan, and R. G. Eckenhoff. 2002. Multiple specific binding targets for inhaled anaesthetics in the mammalian brain. *J. Pharmacol. Exp. Ther.* **300**: 172–179.
71. Eckenhoff, R. G., and J. S. Johansson. 1999. On the relevance of “clinically relevant concentrations” of inhaled anaesthetics in in vitro experiments. *Anesthesiology*. **91**: 856–860.
72. Harrison, N. L. 2000. Ion channels take center stage: twin spotlights on two anaesthetic targets. *Anesthesiology*. **92**: 936–938.
73. Richens, J. L., J. S. Lane, J. P. Bramble, and P. O’Shea. 2015. The electrical interplay between proteins and lipids in membranes. *Biochim. Biophys. Acta.* **1848**: 1828–1836.
74. Allen, J. A., R. A. Halverson-Tamboli, and M. M. Rasenick. 2007. Lipid raft microdomains and neurotransmitter signalling. *Nat. Rev. Neurosci.* **8**: 128–140.
75. Delint-Ramirez, I., E. Fernández, A. Bayés, E. Kicsi, N. H. Komiyama, and S. G. N. Grant. 2010. In vivo composition of NMDA receptor signaling complexes differs between membrane subdomains and is modulated by PSD-95 and PSD-93. *J. Neurosci.* **30**: 8162–8170.
76. Nothdurfter, C., S. Tanasic, B. Di Benedetto, M. Uhr, E-M. Wagner, K. E. Gilling, C. G. Parsons, T. Rein, F. Holsboer, R. Rupprecht, et al. 2013. Lipid raft integrity affects GABAA receptor, but not NMDA receptor modulation by psychopharmacological compounds. *Int. J. Neuropsychopharmacol.* **16**: 1361–1371.
77. Escher, B. I., C. Berger, N. Bramaz, J-H. Kwon, M. Richter, O. Tsinman, and A. Avdeef. 2008. Membrane-water partitioning, membrane permeability, and baseline toxicity of the parasitocides

- ivermectin, albendazole, and morantel. *Environ. Toxicol. Chem.* **27**: 909–918.
78. Gawrisch, K., D. Ruston, J. Zimmerberg, V. A. Parsegian, R. P. Rand, and N. Fuller. 1992. Membrane dipole potentials, hydration forces, and the ordering of water at membrane surfaces. *Biophys. J.* **61**: 1213–1223.
79. Brockman, H. 1994. Dipole potential of lipid membranes. *Chem. Phys. Lipids.* **73**: 57–79.
80. Cladera, J., and P. O'Shea. 1998. Intramembrane molecular dipoles affect the membrane insertion and folding of a model amphiphilic peptide. *Biophys. J.* **74**: 2434–2442.
81. Clarke, R. J. 2001. The dipole potential of phospholipid membranes and methods for its detection. *Adv. Colloid Interface Sci.* **89–90**: 263–281.
82. North, C., and D. S. Cafiso. 1997. Contrasting membrane localization and behavior of halogenated cyclobutanes that follow or violate the Meyer-Overton hypothesis of general anesthetic potency. *Biophys. J.* **72**: 1754–1761.
83. Tang, P., B. Yan, and Y. Xu. 1997. Different distribution of fluorinated anesthetics and nonanesthetics in model membrane: a 19F NMR study. *Biophys. J.* **72**: 1676–1682.
84. Tang, P., J. Hu, S. Liachenko, and Y. Xu. 1999. Distinctly different interactions of anesthetic and nonimmobilizer with transmembrane channel peptides. *Biophys. J.* **77**: 739–746.
85. Tang, P., V. Simplaceanu, and Y. Xu. 1999. Structural consequences of anesthetic and nonimmobilizer interaction with gramicidin A channels. *Biophys. J.* **76**: 2346–2350.
86. Bondarenko, V., V. E. Yushmanov, Y. Xu, and P. Tang. 2008. NMR study of general anesthetic interaction with nAChR beta2 subunit. *Biophys. J.* **94**: 1681–1688.
87. Sarkar, P., and A. Chattopadhyay. 2016. Micellar dipole potential is sensitive to sphere-to-rod transition. *Chem. Phys. Lipids.* **195**: 34–38.
88. Franks, N. P., and W. R. Lieb. 1986. Partitioning of long-chain alcohols into lipid bilayers: implications for mechanisms of general anesthesia (anesthetic target sites/cutoff effects/firefly luciferase). *Proc. Natl. Acad. Sci. USA.* **83**: 5116–5120.
89. Miller, K. W., and L. L. Firestone, J. K. Alifimoff, and P. Streicher. 1989. Nonanesthetic alcohols dissolve in synaptic membranes without perturbing their lipids. *Neurobiology.* **86**: 1084–1087.
90. Ingólfsson, H. I., and O. S. Andersen. 2011. Alcohol's effects on lipid bilayer properties. *Biophys. J.* **101**: 847–855.
91. Chiou, J. S., S. M. Ma, H. Kamaya, and I. Ueda. 1990. Anesthesia cutoff phenomenon: interfacial hydrogen bonding. *Science.* **248**: 583–585.
92. Di Paolo, T., and C. Sandorfy. 1974. Hydrogen bond breaking potency of fluorocarbon anesthetics. *J. Med. Chem.* **17**: 809–814.
93. Wang, H., B. Wang, K. P. Normoyle, K. Jackson, K. Spitzer, M. F. Sharrock, C. M. Miller, C. Best, D. Llano, and R. Du. 2014. Brain temperature and its fundamental properties: a review for clinical neuroscientists. *Front. Neurosci.* **8**: 307.
94. Morris, R. W. 1966. Analgesic and local anesthetic activity of dimethyl sulfoxide. *J. Pharm. Sci.* **55**: 438–440.
95. Galvao, J., B. Davis, M. Tilley, E. Normando, M. R. Duchon, and M. F. Cordeiro. 2014. Unexpected low-dose toxicity of the universal solvent DMSO. *FASEB J.* **28**: 1317–1330.
96. Gibbons, E., K. R. Pickett, M. C. Streeter, A. O. Warcup, J. Nelson, A. M. Judd, and J. D. Bell. 2013. Molecular details of membrane fluidity changes during apoptosis and relationship to phospholipase A(2) activity. *Biochim. Biophys. Acta.* **1828**: 887–895.
97. Mascia, M. P., T. K. Machu, and R. A. Harris. 1996. Enhancement of homomeric glycine receptor function by long-chain alcohols and anaesthetics. *Br. J. Pharmacol.* **119**: 1331–1336.
98. Minami, K., T. W. Vanderah, M. Minami, and R. A. Harris. 1997. Inhibitory effects of anesthetics and ethanol on muscarinic receptors expressed in *Xenopus* oocytes. *Eur. J. Pharmacol.* **339**: 237–244.
99. Yamakura, T., J. M. Lewohl, and R. A. Harris. 2001. Differential effects of general anesthetics on G protein-coupled inwardly rectifying and other potassium channels. *Anesthesiology.* **95**: 144–153.
100. Shiraishi, M., and R. A. Harris. 2004. Effects of alcohols and anesthetics on recombinant voltage-gated Na⁺ channels. *J. Pharmacol. Exp. Ther.* **309**: 987–994.
101. Liachenko, S., P. Tang, G. T. Somogyi, and Y. Xu. 1998. Comparison of anaesthetic and non-anaesthetic effects on depolarization-evoked glutamate and GABA release from mouse cerebrotical slices. *Br. J. Pharmacol.* **123**: 1274–1280.
102. Zidovetzki, R., and I. Levitan. 2007. Use of cyclodextrins to manipulate plasma membrane cholesterol content: evidence, misconceptions and control strategies. *Biochim. Biophys. Acta.* **1768**: 1311–1324.
103. Rehberg, B., B. W. Urban, and D. S. Duch. 1995. The membrane lipid cholesterol modulates anesthetic actions on a human brain ion channel. *Anesthesiology.* **82**: 749–758.
104. Bari, M., N. Battista, F. Fezza, A. Finazzi-Agrò, and M. Maccarrone. 2005. Lipid rafts control signaling of type-1 cannabinoid receptors in neuronal cells. Implications for anandamide-induced apoptosis. *J. Biol. Chem.* **280**: 12212–12220.
105. Weis, R. M., and H. M. McConnell. 1984. Two-dimensional chiral crystals of phospholipid. *Nature.* **310**: 47–49.
106. Lalitha, S., A. Sampath Kumar, K. J. Stine, and D. F. Covey. 2001. Chirality in membranes: first evidence that enantioselective interactions between cholesterol and cell membrane lipids can be a determinant of membrane physical properties. *J. Supramol. Chem.* **1**: 53–61.
107. Kang, L., and T. C. Lubensky. 2017. Chiral twist drives raft formation and organization in membranes composed of rod-like particles. *Proc. Natl. Acad. Sci. USA.* **114**: E19–E27.
108. Freeman, W. R., D-U. Bartsch, A. J. Mueller, A. S. Banker, and R. N. Weinreb. 1998. Simultaneous indocyanine green and fluorescein angiography using a confocal scanning laser ophthalmoscope. *Arch. Ophthalmol.* **116**: 455.
109. Cordeiro, M. F., E. M. Normando, M. J. Cardoso, S. Miodragovic, S. Jeylani, B. M. Davis, L. Guo, S. Ourselin, R. A'Hern, and P. A. Bloom. 2017. Real-time imaging of single neuronal cell apoptosis in patients with glaucoma. *Brain.* **274**: 61–65.
110. Galvao, J., B. M. Davis, and M. F. Cordeiro. 2013. In vivo imaging of retinal ganglion cell apoptosis. *Curr. Opin. Pharm.* **13**: 123–127.
111. Behrooz, A. 2015. Pharmacogenetics and anaesthetic drugs: implications for perioperative practice. *Ann. Med. Surg.* **4**: 470–474.